

Numerically Computing Galois Groups of Minimal Problems

Timothy Duff
 tduff@missouri.edu
 University of Missouri - Columbia
 Columbia, Missouri, USA

ABSTRACT

I discuss a seemingly unlikely confluence of topics in algebra, numerical computation, and computer vision. The motivating problem is that of solving multiples instances of a parametric family of systems of algebraic (polynomial or rational function) equations. No doubt already of interest to ISSAC attendees, this problem arises in the context of robust model-fitting paradigms currently utilized by the computer vision community (namely "Random Sampling and Consensus", aka "RanSaC".) This talk will give an overview of work in the last 5+ years that aspires to measure the intrinsic difficulty of solving such parametric systems, and makes strides towards practical solutions.

ACM Reference Format:

Timothy Duff. 2025. Numerically Computing Galois Groups of Minimal Problems. In *Proceedings of ISSAC 2025 (ISSAC '25)*. ACM, New York, NY, USA, 10 pages. <https://doi.org/XXXXXX.XXXXXXX>

1 INTRODUCTION

This article accompanies an invited tutorial presented at the ISSAC 50th anniversary conference in Guanajuato. It offers expository accounts of algebraic vision [41], Galois groups of polynomial systems [60], and numerical algebraic geometry [4]. Needless to say, the 8-page format prevents treating any one of these topics in-depth. I encourage readers seeking more details to look at the surveys cited above. The main novelty is the synthesis of these three topics.

2 ALGEBRAIC VISION

Every application of algebraic geometry I've ever worked on is motivated by some instance of the following "universal problem": Let $\pi : \mathcal{X} \dashrightarrow \mathbb{C}^m$ be a rational map, \mathcal{X} a variety of unknown states, and $\pi(\mathcal{X}) \subset \mathbb{C}^m$ a space of idealized data. Given a measurement $\tilde{y} \approx y$ of "true" data $y = \pi(x)$, recover $\tilde{x} \in \mathcal{X}$ with $\tilde{x} \approx x$.

Computer vision is replete with such problems. I work over the complex numbers for simplicity. This is bearing in mind, of course, that in practice the input \tilde{y} is real-valued, and that your solution \tilde{x} also better be real if you want anyone to care about your work.

Permission to make digital or hard copies of all or part of this work for personal or classroom use is granted without fee provided that copies are not made or distributed for profit or commercial advantage and that copies bear this notice and the full citation on the first page. Copyrights for components of this work owned by others than the author(s) must be honored. Abstracting with credit is permitted. To copy otherwise, or republish, to post on servers or to redistribute to lists, requires prior specific permission and/or a fee. Request permissions from permissions@acm.org.

ISSAC '25, July 28–August 1, 2025, Guanajuato, Mexico

© 2025 Copyright held by the owner/author(s). Publication rights licensed to ACM. ACM ISBN 978-1-4503-XXXX-X/2025/06...\$15.00
<https://doi.org/XXXXXX.XXXXXXX>

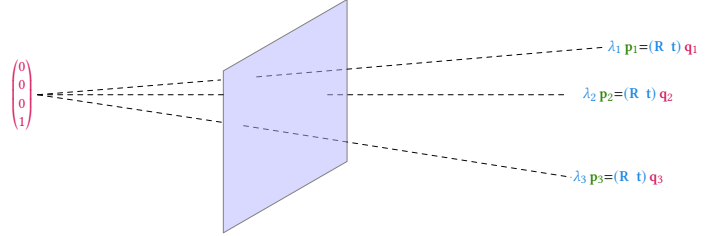


Figure 1: Illustration of Perspective-3-Point: p_i denotes the normalized homogeneous coordinates of a 2D point $y_i \in \mathbb{R}^2$, and λ_i denotes the projective depth of the 3D point q_i (in affine terms, the distance from q_i to the center of projection.)

Example 2.1. The classic "Perspective- n -Point" problem (PnP) can be formulated as follows: fix $q_1, \dots, q_n \in \mathbb{P}(\mathbb{C}^{4 \times 1})$, and define

$$\begin{aligned} \pi : \mathbf{SE}_3 &\dashrightarrow (\mathbb{C}^2)^n & (1) \\ (\mathbf{R} | \mathbf{t}) &\mapsto (\Pi((\mathbf{R} | \mathbf{t})q_1), \dots, \Pi((\mathbf{R} | \mathbf{t})q_n)) \\ \text{where } \Pi(x, y, z) &= (x/z, y/z). \end{aligned}$$

The data q_1, \dots, q_n represent three-dimensional points in homogeneous coordinates, and \mathbf{SE}_3 is the (complexified) special Euclidean group. Here is the problem: given $y_1, \dots, y_n \in \mathbb{C}^2$ and the corresponding q_1, \dots, q_n , find $(\mathbf{R} | \mathbf{t}) \in \mathbf{SE}_3$ such that

$$\pi((\mathbf{R} | \mathbf{t})) \approx (y_1, \dots, y_n). \quad (2)$$

Any discussion of how to define the symbol \approx would lead us too far astray, so let's consider a scenario that is quite natural for the ISSAC community: the existence of an *exact solution*,

$$\pi((\mathbf{R} | \mathbf{t})) = (y_1, \dots, y_n). \quad (3)$$

Counting dimensions, it should come as little surprise that an exact solution exists when $n = 3$ for generic data $(q_1, q_2, q_3, y_1, y_2, y_3)$. This is the hallmark of a *minimal problem*.

P3P, all things considered, is a pretty simple problem, and also a pretty old one, dating back to Lagrange in the 1700s (see [62] for related history.) Thus, it is remarkable that P3P continues to receive considerable attention in recent literature coming from both symbolic computation [27, 30] and computer vision [15, 53].

Minimal problems might seem like a theoretical curiosity—after all, wouldn't you really like to solve the inexact problem (2), for any n ? However, the computer vision community has realized that minimal problems can be a surprisingly effective tool for outlier-robust estimation. To motivate this, note that the inexact formulation of (2) is still rather naive, since it assumes the knowledge of *exact point correspondences*. In reality, these correspondences usually arise as byproducts of image processing or machine learning methods, and as a result are not merely noisy, but often flat out *wrong*.

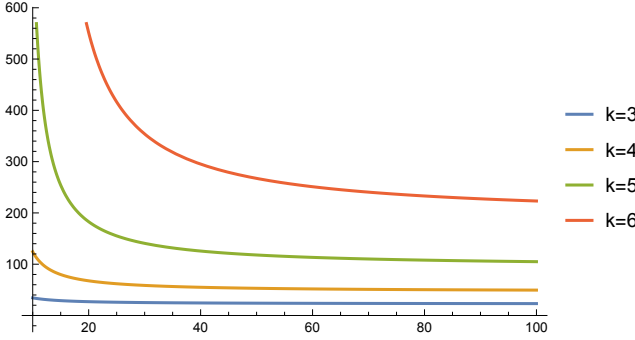


Figure 2: Based on (6), the number of RanSaC trials N needed to find an outlier-free subsample of size k with 95% confidence from $n \in [10, 100]$ total correspondences, with 50% outliers.

To cope with erroneous correspondences, we could try multiple trials in which we solve (2) for different sub-samples of the data; then, using the solutions obtained in each trial, we may attempt to discern which data are erroneous. This is the essential idea behind a popular paradigm known as *Random Sampling and Consensus*, aka *RanSaC*, introduced by Fischler and Bolles in 1981 [28]. Following the more recent work [57], we analyze the complexity of RanSaC in its simplest of forms. Assume we have the following:

- (1) N , the number of trials,
- (2) a working solver for the PkP problem, where k is the number of correspondences used in any of the N trials,
- (3) a “consensus” criterion by which unsampled correspondences are judged to be either consistent or inconsistent with a solution (“inliers” and “outliers”, respectively),
- (4) $s \in (0, 1)$, the desired probability of obtaining an outlier-free sample of k correspondences after N trials.

Let $p \in (0, 1)$ denote the fraction of erroneous correspondences, so that the probability of drawing an all-inlier sample in one trial is

$$P = \frac{\binom{pn}{k}}{\binom{n}{k}}. \quad (4)$$

From our specification above, we should have

$$(1 - P)^N \leq 1 - s, \quad (5)$$

so the number of trials should satisfy

$$N \geq \frac{\log(1 - s)}{\log(1 - P)}. \quad (6)$$

Figure 2 plots the right-hand side of (6) for $s = .95$, $p = .5$, $n \in \{10, \dots, 100\}$ and $k \in \{3, 4, 5, 6\}$. Clearly, fewer trials are needed as we decrease the size of subsamples k . In the case of P3P, $k = 3$ is the absolute minimum number of correspondences we’d need to solve the PkP problem up to finitely-many candidate solutions. Typically, an instance of the P3P problem has more than one plausible solution. Thus, each trial generates multiple candidates that must be scored accordingly inside of the RanSaC loop in order to obtain an unambiguous estimate of the “true” solution. This solution is then refined after running RanSaC, using nonlinear least squares with the associated consensus set. In fact, RanSaC exists in a multitude of different flavors, such as LO-RanSaC [10], which incorporates

such refinement steps into each of the trials. I couldn’t possibly do justice to the vast landscape of different RanSaCs, especially in this short article. Still, regardless of the RanSaC flavor that one uses, the point remains that *the most sample-efficient solvers are minimal*.

Let’s return to P3P—how might we actually solve it? Referring to Figure 1, we’ll put each 2D point $\mathbf{y}_i \in \mathbb{R}^2$ into homogeneous coordinates, $\mathbf{p}_i \in \mathbb{P}(\mathbb{R}^{3 \times 1})$, normalized so that $\mathbf{p}_i^T \mathbf{p}_i = 1$. If $\mathbf{q}_1, \mathbf{q}_2, \mathbf{q}_3$ are expressed in the affine chart where their last coordinates equal 1, then we must have

$$\lambda_i \mathbf{p}_i = (\mathbf{R} | \mathbf{t}) \mathbf{q}_i, \quad i = 1, 2, 3, \quad (7)$$

for some unknown scalar *depths* $\lambda_1, \lambda_2, \lambda_3$. Using the law of cosines, one can obtain a system of three equations in the unknown depths,

$$\begin{aligned} \lambda_1^2 + \lambda_2^2 - 2 \left(\mathbf{p}_1^T \mathbf{p}_2 \right) \lambda_1 \lambda_2 &= (\mathbf{q}_1 - \mathbf{q}_2)^T (\mathbf{q}_1 - \mathbf{q}_2), \\ \lambda_1^2 + \lambda_3^2 - 2 \left(\mathbf{p}_1^T \mathbf{p}_3 \right) \lambda_1 \lambda_3 &= (\mathbf{q}_1 - \mathbf{q}_3)^T (\mathbf{q}_1 - \mathbf{q}_3), \\ \lambda_2^2 + \lambda_3^2 - 2 \left(\mathbf{p}_2^T \mathbf{p}_3 \right) \lambda_2 \lambda_3 &= (\mathbf{q}_2 - \mathbf{q}_3)^T (\mathbf{q}_2 - \mathbf{q}_3). \end{aligned} \quad (8)$$

The system (8) generically has the “expected” $2^3 = 8$ solutions.

Intersecting three quadrics in three unknowns is a special, well-studied problem [44], but P3P is *even more* special. This is because solutions to (8) exist in symmetric pairs, $(\pm \lambda_1, \pm \lambda_2, \pm \lambda_3)$. It’s also quite reasonable to assume that the depths are nonzero. Introducing new unknowns $(\rho_1, \rho_2) = (\lambda_1/\lambda_3, \lambda_2/\lambda_3)$, we deduce from (8) that

$$\begin{aligned} d_{13} \left(\rho_1^2 + \rho_2^2 + c_{12} \rho_1 \rho_2 \right) &= d_{12} \left(1 + \rho_1^2 + c_{13} \rho_1 \right), \\ d_{23} \left(\rho_1^2 + \rho_2^2 + c_{12} \rho_1 \rho_2 \right) &= d_{12} \left(1 + \rho_2^2 + c_{23} \rho_2 \right), \end{aligned} \quad (9)$$

where $c_{ij} = \mathbf{p}_i^T \mathbf{p}_j$ and $d_{ij} = (\mathbf{q}_i - \mathbf{q}_j)^T (\mathbf{q}_i - \mathbf{q}_j)$. In other words, P3P reduces to intersecting *two plane conics*!

How is Galois theory relevant to this example? Well, two generic plane conics intersect in four points, and if these conics are defined over \mathbb{Q} , then the intersection points have coordinates which are algebraic numbers of degree 4. In principle, these coordinates could be represented exactly on a computer by their quartic minimal polynomials. On the other hand, Galois theory provides us with the following mantra: *solving the quartic can be achieved by solving an auxiliary cubic and auxiliary quadratics*. For P3P, this mantra manifests as follows: consider the *conic pencil*

$$(\rho_1 \quad \rho_2 \quad 1) (tC_1 + (1 - t)C_2) \begin{pmatrix} \rho_1 \\ \rho_2 \\ 1 \end{pmatrix} = 0, \quad (10)$$

where C_1 and C_2 are 3×3 symmetric matrices representing the two conics (9). By genericity, we may assume C_2 is invertible; if the two conics intersect at a point (ρ_1, ρ_2) in the pencil, then the corresponding value of t must solve the 3×3 eigenvalue problem

$$\det \left(I - t \left((C_2 - C_1)^{-1} C_2 \right) \right) = 0. \quad (11)$$

Equation (11) is our auxiliary cubic. For each of its roots t , we may form the rank-2 symmetric matrix

$$tC_1 + (1 - t)C_2, \quad (12)$$

representing a degenerate conic. Generically, this is the union of two lines which can be found using the formulas of [55, Ch. 12]; these involve taking the adjugate of (12) and working in a suitable

quadratic extension of the field $\mathbb{Q}(t)$. Intersecting these two lines with one of the original conics C_i recovers the four intersection points (p_1, p_2) . At last, one more quadratic extension recovers the unknown depths $(\lambda_1, \lambda_2, \lambda_3)$, and from there it is only a matter of simple algebra to recover the unknowns R and t . This type of “cubic solution” to P3P has long been known—see [35] for a review of early work, and [15, 53] for more recent developments.

The name *algebraic vision* [41] has recently been coined to describe the interface between algebraic geometry (often of a computational flavor) and problems like P3P which arise in computer vision. This algebraic perspective has produced novel insights and improved solutions to many classical instances of the previously-described “universal problem”: for example, *camera resectioning / absolute pose* [12, 37, 43], *3D point triangulation* [24, 45, 51], *3D reconstruction / relative camera pose* [3, 18, 26, 36, 38, 38–40], and *autocalibration* [11, 42, 46]. From a theoretical angle, it is interesting to answer fundamental algebro-geometric questions about these problems and how they relate; see [1] for one recent overview. From a more practical angle, algebraic vision derives much of its mandate from the study of minimal problems, which may lead to more efficient minimal solvers.

The PnP problem is nothing more than the resectioning problem for a calibrated perspective camera, given 3D-2D point matches. This is generalized in the next example.

Example 2.2. Given p 3D-2D point matches and l 3D-2D line matches, the map defining the calibrated resectioning problem is

$$\pi' : \text{SE}_3 \dashrightarrow (\mathbb{P}^2)^p \times \text{Gr}(\mathbb{P}^1, \mathbb{P}^2)^l \quad (13)$$

$$(R, t) \mapsto \left((R \ t) q_1, \dots, (R \ t) q_p, \wedge^2 (R \ t) \ell_1, \dots, \wedge^2 (R \ t) \ell_l \right).$$

where \wedge denotes the exterior square of a linear map, and we have fixed $q_1, \dots, q_p \in \mathbb{P}^3$ (as in PnP) and lines $\ell_1, \dots, \ell_l \in \text{Gr}(\mathbb{P}^1, \mathbb{P}^3)$. This generalized resectioning problem is minimal when $p + l = 3$, and $(p, l) = (3, 0)$ is just P3P in projective coordinates. In the computer vision literature, the minimal cases involving lines have been studied in a number of previous works.

Solvers for the “pure lines” case $(0, 3)$ based on the intersection of three quadrics date back to the 1980s [14]. In comparison with P3P, it is natural to ask: can we also reduce to the problem of intersecting two conics? This is indeed possible when the lines are in certain special positions (eg. three lines meeting at a point [65].) However, analyzing the Galois group associated to the problem, which turns out to be the full-symmetric group S_8 [20, 37], shows that *such a reduction is generally impossible*.

The “mixed cases” $(2, 1)$ and $(1, 2)$ have also been studied. For example, [54] proposes a pipeline that uses such solvers in the context of urban localization tasks. These solvers were already quite efficient, but were later significantly improved in [37]. These improvements exploited the fact that both of these problems *decompose* into subproblems, as suggested by Galois group computation.

We now move from resectioning onto harder problems.

Example 2.3. The *reconstruction problem* asks us to recover n 3D points and m cameras from projections. Unlike resectioning, $m \geq 2$ cameras are needed in order to solve this problem. This is for the same reason humans need two eyes to perceive depth; see Figure 3

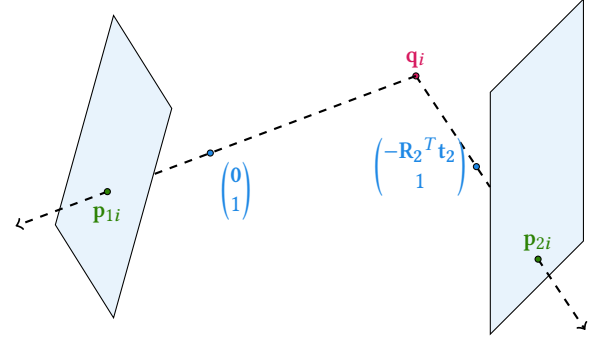


Figure 3: Geometry of the calibrated stereo pair (18).

for an illustration of the $m = 2$ “stereo vision” problem. To simplify the exposition, we assume each camera is *calibrated*—that is, an element $A \in \text{SE}_3$. Thus, inverting the map

$$\Psi_{m,n} : \text{SE}_3^m \times (\mathbb{P}^3)^n \dashrightarrow (\mathbb{P}^2)^{mn} \quad (14)$$

$$(A_1, \dots, A_m, q_1, \dots, q_n) \mapsto (A_1 q_1, \dots, A_m q_n). \quad (15)$$

seems to be a natural formulation for the reconstruction problem. However, for any m and n , the map (14) has positive-dimensional fibers, due to the action of the *similarity group*

$$\mathcal{S}_3 = \left\{ H \in \text{PGL}_4 \mid H \sim \begin{pmatrix} R & t \\ 0 & s \end{pmatrix}, \quad (R \mid t) \in \text{SE}_3, \quad s \in \mathbb{C}^* \right\},$$

$$H \cdot (A_1, \dots, A_m, q_1, \dots, q_n) = (A_1 H^{-1}, \dots, A_m H^{-1}, H q_1, \dots, H q_n).$$

(Here, and later, \sim denotes equality up to scale.)

The ambiguity of solutions created by this group action is a natural one: reconstruction from calibrated cameras is only possible up to a choice of world coordinates and global scaling. Thus, we may reformulate reconstruction as inverting the rational map

$$\widetilde{\Psi}_{m,n} : (\text{SE}_3^m \times (\mathbb{P}^3)^n) / \mathcal{S}_3 \dashrightarrow (\mathbb{P}^2)^{mn} \quad (16)$$

$$(A_1, \dots, A_m, q_1, \dots, q_n) \mapsto (A_1 q_1, \dots, A_m q_n), \quad (17)$$

where the quotient may be understood as the “rational quotient” of Rosenlicht [56]. A typical trick used to model this quotient is to fix the first two cameras as follows:

$$A_1 \sim (I \mid 0), \quad A_2 \sim (R_2 \mid t_2), \quad t_2 = \begin{pmatrix} t_1 \\ t_2 \\ 1 \end{pmatrix}. \quad (18)$$

A minimal case for inverting (16) occurs when $(m, n) = (2, 5)$: this is expected, since both domain and codomain have dimension

$$2 \cdot 6 + 5 \cdot 3 - 7 = 2 \cdot 5 \cdot 2 = 20.$$

In fact, a similar count shows that this is the *only* minimal case for inverting $\widetilde{\Psi}_{m,n}$. Reconstructing configurations of points and lines, however, has a much richer story (see eg. [18, 19, 25]).

Let us explain the usual equations for reconstructing 5 points in 2 views, and how Galois theory enters the picture. Suppose

$$\Psi_{2,5}(A_1, A_2, q_1, \dots, q_5) = (p_{11}, \dots, p_{25}), \quad (A_1, A_2) \text{ as in (18).}$$

For the stereo pair (18), we then have for $i = 1, \dots, 5$ that

$$\mathbf{p}_{1i} \sim \mathbf{A}_1 \mathbf{q}_i \Rightarrow \mathbf{p}_{2i} \sim \mathbf{A}_2 \mathbf{q}_i \sim \mathbf{R} \mathbf{p}_{1i} + \mathbf{t} \Rightarrow \mathbf{p}_{2i}^T ([\mathbf{t}] \times \mathbf{R}) \mathbf{p}_{1i} = 0, \quad (19)$$

where $[\mathbf{t}] \times$ is the 3×3 skew symmetric matrix representing the cross-product as a linear map $\mathbb{C}^3 \ni \mathbf{p} \mapsto \mathbf{t} \times \mathbf{p} \in \mathbb{C}^3$.

The matrix $[\mathbf{t}] \times \mathbf{R}$ is known in computer vision as the *essential matrix* associated to the stereo pair (18). The *Nistér-Stewénius five-point algorithm* [61] reconstructs five points in three views by using the equations (19) to derive a degree-10 polynomial, whose roots generically determine 10 distinct complex-valued essential matrices. Each essential matrix, in turn, gives rise to two possibilities for the stereo pair (18). Finally, 3D points \mathbf{q}_i are determined as the intersection of two lines as in Figure 3. Thus, just like in Examples 2.1 and 2.2, the five-point algorithm proceeds by decomposing the reconstruction problem into simpler algebraic subproblems. This observation is plainly seen from the Galois group's action on the 20 solutions.

So far, we have exclusively treated calibrated pinhole cameras. Algebraic vision, however, has a lot to offer to other camera models involving polynomial, rational, and even algebraic functions. We conclude this section with one such example.

Example 2.4. One reason to look beyond the pinhole camera model is the phenomenon of *radial distortion*, in which the magnification of an image increases or decreases away from a fixed point (the *center of distortion*.) A large number of models have been proposed for modeling radial distortion: for example, under the so-called *division model* [29], we have

$$\mathbf{A} \mathbf{q} \sim \mathbf{p} \sim \begin{pmatrix} y_1 \\ y_2 \\ 1 + \rho(y_1^2 + y_2^2) \end{pmatrix}, \quad (20)$$

where now $(y_1, y_2) \in \mathbb{C}^2$ represents the measured 2D point, and ρ is a new, unknown *radial distortion parameter*. Note that, under this model, it is not straightforward to write the image point (y_1, y_2) as a function of the 3D point \mathbf{q} and the camera parameters \mathbf{A}, ρ . However, if our true goal is to recover \mathbf{A} and \mathbf{q} , then one can make use of the *radial camera model* [38]. Here, we simply focus on the first two rows of (20), which do not involve ρ : we have

$$\tilde{\mathbf{A}} \mathbf{q} \sim \begin{pmatrix} y_1 \\ y_2 \end{pmatrix},$$

where $\tilde{\mathbf{A}} : \mathbb{P}^3 \dashrightarrow \mathbb{P}^1$ is the *calibrated radial camera* associated to the pinhole camera \mathbf{A} . Thus, calibrated radial cameras have the form

$$\tilde{\mathbf{A}}_i = \begin{pmatrix} \mathbf{r}_{i1}^T & t_{i,1} \\ \mathbf{r}_{i2}^T & t_{i,2} \end{pmatrix}, \quad \mathbf{r}_{i1}^T \mathbf{r}_{i1} = \mathbf{r}_{i2}^T \mathbf{r}_{i2} = 1, \quad \mathbf{r}_{i1}^T \mathbf{r}_{i2} = 0. \quad (21)$$

Similarly to (16), we may try to invert a reconstruction map with codomain $(\mathbb{P}^1)^{mn}$, and whose domain consists \mathcal{S}_3 -orbits of pairs consisting m -tuple of calibrated radial cameras and an n -tuple of 3D points to their projections. Analogously to (18), we we may assume

$$\tilde{\mathbf{A}}_1 \sim \begin{pmatrix} 1 & 0 & 0 & 0 \\ 0 & 1 & 0 & 0 \end{pmatrix}, \quad \tilde{\mathbf{A}}_2 \sim \begin{pmatrix} \mathbf{r}_{21}^T & 0 \\ \mathbf{r}_{22}^T & 1 \end{pmatrix}. \quad (22)$$

In this case, we haven't entirely resolved the \mathcal{S}_3 -ambiguity; the variety of all calibrated radial camera pairs $(\tilde{\mathbf{A}}_1, \tilde{\mathbf{A}}_2)$ having the form (22) is stabilized by the elements $\mathbf{H} = \text{diag}(1, 1, \pm 1, \pm 1) \in \mathcal{S}_3$.

The first minimal case for radial camera reconstruction occurs when $(m, n) = (4, 13)$: the problem is to solve

$$\tilde{\mathbf{A}}_i \mathbf{q}_j \sim \mathbf{y}_{ij} \quad \forall 1 \leq i \leq 4, 1 \leq j \leq 13, \quad (23)$$

where the data $\mathbf{y}_{ij} \in \mathbb{P}^1$ are given. Taken together, equations (21), (22) and (23) are naturally formulated as a system of polynomials. A numerical monodromy computation in [38] determined this system to have 3584 solutions. This might seem like terrible news. However, as a byproduct of this same computation, one obtains a permutation group which serves as a good proxy for the true Galois group. The structure of this permutation group indicates that the solutions are highly structured: indeed, up to \mathcal{S}_3 -equivalence, there are merely $3584/16 = 224$ solutions. What's more, the reconstruction problem decomposes further into sub-problems like the five-point problem of Example 2.3. The natural analogue of the essential matrix for this problem is the *radial quadrifocal tensor*: as it turns out, the 896 \mathcal{S}_3 -orbits map onto 56 = $224/4$ PGL_4 -orbits of *uncalibrated* reconstructions, which in turn map onto 28 radial quadrifocal tensors. By carefully tracing through the associated subproblems, one may recover all 3584 solutions via a numerical homotopy continuation method that tracks just 28 paths. Needless to say, this is a significant improvement! We refer to [38] for many more details.

Now that we've seen examples of minimal problems, let's give a general overview of their Galois groups and how to compute them.

3 GALOIS GROUPS OF POLYNOMIAL SYSTEMS

The minimal problems of the previous section all adhere to a common setup: let $\mathcal{X} \subset \mathbb{C}^m \times \mathbb{C}^n$ be a variety whose points are *problem-solution* pairs, for which we make the following assumptions:

- (1) The projection $\pi : \mathcal{X} \rightarrow \mathbb{C}^m$ onto the space of problems is dominant and generically d -to-1 for some $d \geq 1$, and
- (2) The variety \mathcal{X} is *irreducible*.

Solving a generic instance $\mathbf{z} \in \mathbb{C}^m$ of a minimal problem for us then simply means enumerating all d solutions in the fiber $\pi^{-1}(\mathbf{z})$. We note that assumption 2, although seemingly restrictive, is satisfied by nearly all minimal problems encountered in practice.

It is often more convenient to describe the map π abstractly, with the understanding that the local description above is equivalent. To be more precise, suppose we are given given an “abstract” *branched cover* $\pi' : \mathcal{X} \dashrightarrow \mathcal{Z}$: that is, a dominant map between irreducible complex algebraic varieties of dimension m . For minimal problems, one can produce explicit birational isomorphisms $t : \mathcal{X} \dashrightarrow \mathcal{Z}$ and $b : \mathbb{C}^m \dashrightarrow \mathcal{Z}$ with $\pi' \circ t$ equal to $b \circ \pi$ on a dense common domain of definition $\mathcal{U} \subset \mathcal{X}$. In general, I would like to advocate the following philosophy: *minimal problems are branched covers, and one should try to characterize their intrinsic complexity using birational invariants*. For example, the “abstract” P3P map π' of (13) with $(p, l) = (3, 0)$ is birationally-equivalent to a “problem-solution pair” map $\mathcal{X} \rightarrow \mathbb{C}^9 \times \mathbb{C}^6$ associated to the system (8). Similarly, the “abstract” quotient map (16) has many equivalent models.

The overarching invariant, as you would probably expect, is the *Galois group of the minimal problem*. Letting \mathcal{K} denote the normal closure of the rational function field $\mathbb{C}(\mathcal{X})$ and \mathcal{F} the function field of \mathbb{C}^m , this is simply the group $\mathcal{G} = \text{Gal}(\mathcal{K}/\mathcal{F})$.

The Galois group encodes several more invariants of a minimal problem, via its guises as both an abstract group and as a permutation group acting on the solution set $\pi^{-1}(z)$: mainly,

1. The *degree* / generic number of complex solutions d : when we compute G numerically, we typically obtain explicit permutations of the solution set. Abstractly, d is the index of any *point stabilizer* in G (which stabilizes a single solution.)
2. The *deck transformation group*, which may loosely be understood as the minimal problem's "symmetry group" [21]. Abstractly, this is the centralizer of G in S_d . For example, the P3P system (8), the deck transformation group is $\mathbb{Z}/2\mathbb{Z}$, corresponding to the sign-symmetry $\lambda_i \mapsto -\lambda_i$.
3. *Decomposability*: does π factor as a composition of lower-degree maps? Using [8, Proposition 1], this is equivalent to asking whether or not G acts *imprimitively*, ie. whether it preserves a nontrivial partition of the solution set—or abstractly, whether point stabilizers are maximal subgroups.
4. An invariant which I have recently proposed calling the *Galois width* [16]: this is the quantity

$$gw(G) = \min_{\substack{\text{unrefinable subgroup chains} \\ \text{id} = H_m \leq \dots \leq H_0 = G}} \left(\max_{0 \leq i < m} [H_i : H_{i+1}] \right). \quad (24)$$

The definition of the Galois width is motivated by a simple, exact computation model: to compute an algebraic number α in m steps,

- (1) Initialize $\mathbb{F}_0 \leftarrow \mathbb{Q}$
- (2) For $i = 1, \dots, m$, either
 - do arithmetic in $\mathbb{F}_i \leftarrow \mathbb{F}_{i-1}$, OR
 - compute a root of a polynomial: formally, extend the working field $\mathbb{F}_i \leftarrow \mathbb{F}_{i-1}(\beta)$
- (3) Output: $\alpha \in \mathbb{F}_m$

It is natural to assign a cost of $[\mathbb{F}_i : \mathbb{F}_{i-1}]$ to each step of the algorithm. If G is the Galois group of the minimal polynomial of α , then $gw(G)$ measures the "minimax" cost which minimizes the cost of the most costly step in any such algorithm computing α . [16]

Computing Galois width is typically straightforward when G is known, due to the following results.

THEOREM 3.1 (PROPERTIES OF GALOIS WIDTH (D '25)). *For any finite group G , the following properties hold:*

- $gw(H) \leq gw(G)$ for any subgroup $H \leq G$.
- $gw(G) = \max(gw(N), gw(G/N))$ whenever $N \trianglelefteq G$.
- For any composition series $\text{id} = N_m \trianglelefteq N_{m-1} \trianglelefteq \dots \trianglelefteq N_0 = G$,

$$gw(G) = \max_{0 \leq i < m} gw(N_i/N_{i+1}).$$

- If G is simple, then

$$gw(G) = \min_{H < G} [G : H].$$

- For any prime p , we have $gw(\mathbb{Z}/p\mathbb{Z}) = p$.

- For any $n \geq 1$, we have $gw(S_n) = gw(A_n) = \begin{cases} 3 & \text{if } n = 4, \\ n & \text{else.} \end{cases}$

Galois width provides one (by no means the only) measure for the intrinsic difficulty of solving minimal problems. Computing it has already led in some cases to more efficient minimal solvers than previously known [36, 37]: it seems likely that this trend will continue. Let's review the previous section's examples.

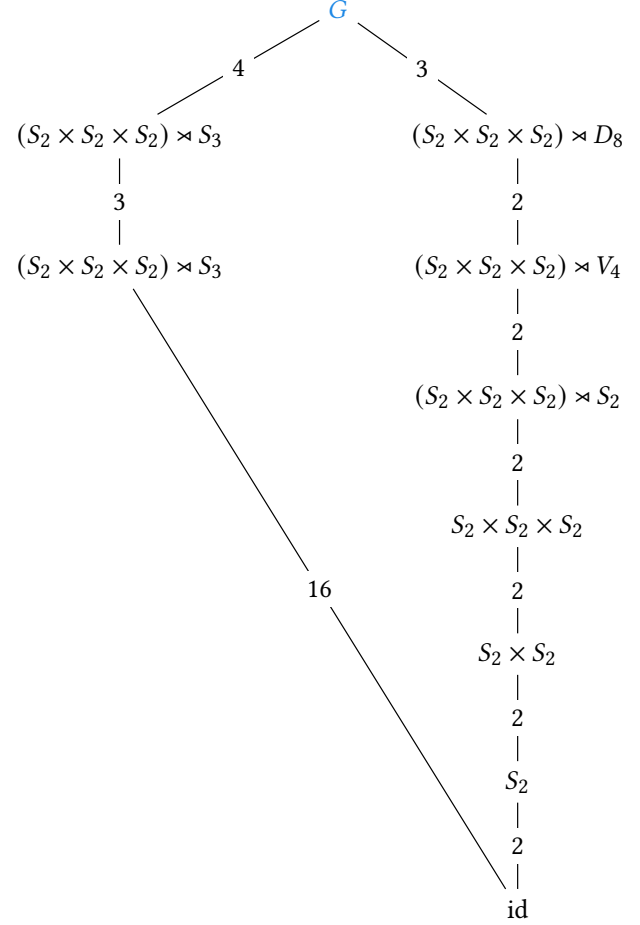


Figure 4: Two subgroup chains in the Galois group of P3P.

Example 3.2. The P3P problem of (2.1) has Galois width 3. This observation relates to [20, §3], where it was noted that the Galois group of this problem is the group of all even permutations of eight letters which preserve a fixed partition into four blocks of size two,

$$G = (S_2 \wr S_4) \cap A_8 = (S_2 \times S_2 \times S_2) \rtimes S_4.$$

The chain of subgroups which attains the minimum in (24) is shown on the right of Figure 4. The (refinable) chain on the left illustrates that chains of subgroups above the point stabilizers

$$(S_2 \times S_2) \rtimes S_3 \leq G$$

are *not* generally sufficient to determine $gw(G)$. In other words, the Galois width measures more than decomposability.

Moving along to the absolute pose problems of Example 2.2: P3P1L has degree 4 but Galois width 2, P1P2L has degree 8 but Galois width 3, and P3L has both degree and Galois width 8.

The five-point relative pose problem of Example 2.3 has degree 20 and Galois width 10, which shows that the Nistér-Stewénius method is algebraically optimal. This agrees with the results of [52], which pioneered the computation of minimal problems' Galois groups. In fact, the Galois groups used in that work were *arithmetic* Galois groups, as opposed to the geometric Galois groups considered in this

survey. These were computed by traditional methods of symbolic computation. The relationship between these results is discussed in [16, §3]—suffice it to say that, even if one is ultimately interested in arithmetic Galois groups, the numerical heuristics which we later describe can be a helpful tool.

Finally, the radial camera reconstruction problem of Example 2.4 has Galois width 28, compared to a naive degree of 3584. This (admittedly extreme) shows the potential payoff of probing the structure of minimal problems through the Galois-theoretic lens.

4 NUMERICALLY COMPUTING MONODROMY

The previous section alluded to an action of a minimal problem's Galois group G on the set of solutions $\pi^{-1}(z) \subset X \subset \mathbb{C}^m \times \mathbb{C}^n$ for a generic problem instance z . This is the *monodromy action*. In practice, this may be computed using *parameter homotopy* [59, Ch. 7], a general framework for numerical homotopy continuation methods. The basic approach requires the following:

- (1) A *fabrication procedure* that produces (numerical approximations of) generic problem-solution-pairs, $(z, x) \in X$, and
- (2) equations $f_1(x; z), \dots, f_n(x; z)$ which locally define X , ie.

$$\text{rank} \left(\frac{\partial f_i}{\partial x_j} \right) \Big|_{(z, x)} = n, \quad \text{for any generic sample } (z, x) \in X.$$

Remark 1. The local equations in (2) above may be polynomial or rational functions. See eg. [23, 63] for two examples of applications where the latter choice is much more convenient.

Remark 2. If we are given local equations, why not just use Newton's method as the fabrication procedure? This often works, but *it is not guaranteed, especially if the vanishing locus $V(f_1, \dots, f_n)$ has irreducible components other than X* . When people complain to me that monodromy isn't solving their problem, they are usually either (a) trying to solve a non-minimal problem, or (b) overlooking this particular subtlety. The takeaway here is: when in doubt, fabricate!

Remark 3. Although minimal problems are locally defined by n equations in unknowns, globally one may need more than n equations. This is not really a problem, because the fabrication procedure should ensure that all equations are (approximately) satisfied, and any full-rank square submatrix of the Jacobian yields suitable local equations. In practice, one should search for such a submatrix carefully—the package `MonodromySolver` [17] implements an effective greedy strategy.

Once the basic requirements (1) and (2) are in place, we are ready to "do monodromy." Start by fabricating a problem-solution pair $(z_0, x_0) \in X$. Then, generate a new generic problem instance $z_1 \in \mathbb{C}^m$, and two analytic paths $\phi_i : [0, 1] \rightarrow \mathbb{C}^m$, $i = 1, 2$, such that the following hypotheses hold:

- (1) $\phi_i(0) = z_0$,
- (2) $\phi_i(1) = z_1$, and
- (3) for all $t \in [0, 1]$, the fiber $\pi^{-1}(\phi_i(t))$ consists of d distinct, isolated points.

The path ϕ_0 determines a *parameter homotopy*

$$H_0(x; t) = \begin{pmatrix} f_1(x; \phi_0(t)) \\ \vdots \\ f_n(x; \phi_0(t)) \end{pmatrix}, \quad (25)$$

to which we associate the initial value problem [59, Ch. 2]

$$x'(t) = - \left(\frac{\partial H_0}{\partial x} \right)^{-1} \frac{\partial H_0}{\partial t}, \quad x(0) = x_0. \quad (26)$$

By our hypotheses on ϕ_0 , this initial value problem admits a local *solution function* $x(t)$, and we may check that $H(x(t); t) = 0$ for all $t \in [0, 1]$. Thus, numerically integrating (26) produces an (approximation of) a solution x_1 to the problem z_1 . This is called *path-tracking*, and implemented with a predictor-corrector scheme.

Remark 4. By construction, $x_1 = x(1)$ satisfies the system

$$f_1(x; z_1) = \dots = f_n(x; z_1) = 0.$$

But one can say more: our hypotheses ensure that $(z_1, x_1) \in X$. Nevertheless, this property may silently fail when tracking paths, due to the well-known phenomenon of *path-jumping*. Thus, it can be helpful to know more about the equations defining X globally, or to play with the various path-tracking tolerances. Another possibility is *certified* path-tracking: based on last year's ISSAC paper [34], this should be doable for moderately-sized minimal problems.

Once we have *two* problem-solution pairs $(z_0, x_0), (z_1, x_1) \in X$, we can use ϕ_1 to construct a second parameter homotopy and track the solution x_1 back to a solution of z_0 . The pair (ϕ_0, ϕ_1) determines a *monodromy loop* in the space of problems, that induces a permutation of the solution set of $\pi^{-1}(z_0)$.

Of course, we really want path-tracking to produce *new* solutions, or to somehow be confident that there are none left to find. Here are some practical strategies used for cooking up monodromy loops:

- (1) Often (eg. for all problems in Section 2), X is invariant under a group action $G \curvearrowright X$; fixing $g_0, g_1 \in G$, we may take

$$\phi_i(t) = (1-t)z_i + g_i \cdot t z_{1-i}. \quad (27)$$

Ideally, for generic $g_0, g_1 \in G$ our hypotheses on $\phi_i(t)$ are satisfied; a particular case of this is the well-known γ -trick. [59, Ch. 8] Support for constructing this type of monodromy loop is provided by the `MonodromySolver` option `Randomizer`.

- (2) ("Triangle loops") Rather than chaining two parameter homotopies $z_0 \rightsquigarrow z_1 \rightsquigarrow z_0$, one can chain instead chain three parameter homotopies $z_0 \rightsquigarrow z_1 \rightsquigarrow z_2 \rightsquigarrow z_0$ using three linear segments like (27), without the need for a group action.
- (3) More generally, the approach of [17] constructs a *graph of homotopies*, whose cycles can be used to construct generators of the monodromy group. This graph allows loops to be re-used, which is much more efficient than cooking up new loops "on the fly." These ideas have proven useful in both the `MonodromySolver` implementation and subsequent `HomotopyContinuation.jl` package [6].

Remark 5. The "straight-line" homotopy often used to introduce homotopy continuation is not equivalent to the parameter homotopy (25) using the linear segment (27). This is because the equations $f_i(x; z)$ may not depend linearly on the parameters z .

Remark 6. A (non-certified) stopping criterion for tracking monodromy loops can be provided by the trace test. In its most general form [48], this can be inefficient, as it requires solving another system with many more solutions. In practice, it is more common to stop once some fixed number of loops fails to make progress. In

the framework of [17], one may require that all solutions in the homotopy graph have been tracked along all possible edges.

The use of the monodromy action in computational algebra has been widespread, with applications like computing Riemann matrices of algebraic curves [13], polynomial factorization [31], and numerical irreducible decomposition [58]. An early reference applying these heuristics to compute geometric Galois groups in Schubert calculus is [49]. Currently, these heuristics are implemented in the publicly-available software packages `MonodromySolver`, part of the computer algebra system `Macaulay2` [32], and `HomotopyContinuation.jl` [6].

Remark 7. Finally, it is worthwhile to clear up one last occasional misconception: monodromy is mostly useful for constructing *start systems*, not for solving target systems. The latter are best dealt with via subsequent parameter homotopy runs (eg. solving a real-valued instance of a minimal problem.) As Example 2.4 illustrates, fully exploiting monodromy loops so as to compute the problem's Galois group can provide a useful tool for optimizing the number of paths tracked by such a homotopy.

5 EXAMPLE WITH CODE

Finally, we'll look at the example of the five-point problem discussed in Example 2.3. We will demonstrate the numerical monodromy heuristic for computing its Galois group, and how to use this information to efficiently solve a real-valued problem instance. The code has been developed to run in `Macaulay2` [32] (version 1.25.06), and the Galois group is analyzed with `GAP` [33] (version 4.14.0.) I encourage the reader to try running this code, or translating it to work with their preferred software package.

We begin by loading the `MonodromySolver` package, and setting up variables (solutions), parameters (problems), and equations, namely (19). We assume the fixed camera pair (18).

```
needsPackage "MonodromySolver";
unknowns = gateMatrix{toList vars(t_1,t_2,r_(1,1)..r_(3,3))};
params = gateMatrix{toList vars(p_(1,1,1)..p_(2,5,3))};
R = matrix for i from 1 to 3 list for j from 1 to 3 list r_(i,j);
I = gateMatrix id_(CC^3);
rotationEqs = flatten entries(R * transpose R - I) | {det R - 1};
E = matrix{{0,-1,t_2},{1,0,-t_1},{-t_2,t_1,0}} * R;
pts1 = for i from 1 to 5 list matrix for j from 1 to 3 list {p_(1,i,j)};
pts2 = for i from 1 to 5 list matrix for j from 1 to 3 list {p_(2,i,j)};
ptEqs = apply(pts1,pts2, (p1,p2) -> transpose p2 * E * p1);
```

The equations above are implemented as straight-line programs. This uses the package `SLPexpressions`, part of a larger constellation of numerical algebraic geometry packages in `Macaulay2` [47]. We use the command `compress` to remove superfluous operations from these straight-line programs, and collect all equations into an instance of the datatype `GateSystem`.

```
eqs = gateMatrix{rotationEqs | apply(ptEqs, e -> compress e_(0,0))};
G = gateSystem(params, unknowns, transpose eqs)
```

The last line produces the following output:

```
o12 = gate system: 11 input(s) --> 15 output(s) (with 30 parameters)
o12 : GateSystem
```

Next, we implement a procedure that fabricates a generic problem-solution pair. This relies on Cayley's birational parameterization of 3×3 rotation matrices,

$$\mathbb{C}^3 \ni \mathbf{t} \mapsto (\mathbf{I} - [\mathbf{t}] \times)(\mathbf{I} + [\mathbf{t}] \times) \in \mathrm{SO}_3. \quad (28)$$

```
fabricate = () -> (
  p1s := apply(5, i -> random(CC^3, CC^1));
  R := random(CC^3, CC^3);
  R = R - transpose R;
  R = (id_(CC^3) - R)^(-1) * (id_(CC^3) + R);
  t := random(CC^2,CC^1) || matrix{{1}};
  p2s := apply(p1s, p -> R * p + t);
  x0 := point{{t_(0,0),t_(1,0)} | flatten entries R};
  z0 := point transpose fold(p1s | p2s, (a, b) -> a||b);
  (z0, x0)
)
```

Next, fabricate a problem-solution pair, and verify that our equations indeed (1) are approximately zero, and (2) locally define the incidence variety X . To aid reproducibility, we set a random seed:

```
setRandomSeed 2025;
(z0, x0) = fabricate();
norm evaluate(G, z0, x0)
numericalRank evaluateJacobian(G, z0, x0)
```

The last two lines generate the following output:

```
i16 : norm evaluate(G, z0, x0)
o16 = 2.598965467441789e-15
o16 : RR (of precision 53)
i17 : numericalRank evaluateJacobian(G, z0, x0)
o17 = 11
```

Since we have more equations than unknowns, we use the function `squareUp` to obtain a square subsystem of 11 local equations. Then, we can finally run monodromy:

```
Gs = squareUp(z0, x0, G);
(V, npaths) = monodromySolve(Gs, z0, {x0}, NumberOfNodes => 5);
monodromyGroup(V.Graph, FileName => "5pt.g");
```

The last line writes a file which can be read by `GAP` [33], containing 19 permutations in the Galois group of the five-point problem:

```
p0:= PermList([18, 5, 15, 10, 3, 11, 8, 9, 19, 6, 20, 13, 14, 1, 17, 7, 4, 16, 12, 2]);
p1:= PermList([5, 3, 6, 1, 2, 16, 11, 4, 17, 9, 18, 14, 12, 8, 13, 15, 19, 20, 7, 10]);
p2:= PermList([1, 6, 11, 2, 5, 3, 16, 14, 10, 4, 7, 8, 13, 9, 15, 12, 18, 17, 19, 20]);
p3:= PermList([18, 11, 8, 16, 2, 13, 10, 5, 1, 7, 15, 9, 12, 6, 17, 4, 3, 14, 19, 20]);
p4:= PermList([16, 7, 17, 19, 1, 13, 14, 5, 9, 3, 11, 10, 15, 18, 4, 20, 6, 8, 12, 2]);
p5:= PermList([11, 1, 3, 2, 16, 6, 10, 8, 5, 7, 13, 9, 4, 14, 15, 12, 18, 17, 19, 20]);
p6:= PermList([3, 6, 5, 20, 16, 18, 10, 17, 1, 7, 15, 8, 4, 13, 14, 19, 2, 12, 9, 11]);
p7:= PermList([6, 9, 10, 2, 19, 1, 5, 15, 16, 13, 4, 11, 20, 7, 8, 12, 18, 17, 14, 3]);
p8:= PermList([5, 3, 6, 1, 2, 16, 11, 4, 17, 9, 18, 14, 12, 8, 13, 15, 19, 20, 7, 10]);
p9:= PermList([9, 16, 18, 7, 15, 13, 8, 5, 3, 6, 14, 4, 1, 17, 11, 10, 19, 20, 12, 2]);
p10:= PermList([15, 9, 14, 18, 8, 7, 16, 10, 12, 4, 2, 11, 6, 3, 1, 17, 13, 5, 20, 19]);
p11:= PermList([15, 13, 2, 11, 8, 18, 3, 17, 4, 14, 16, 5, 6, 12, 1, 9, 19, 20, 10, 7]);
p12:= PermList([15, 14, 12, 4, 19, 18, 13, 17, 7, 5, 10, 3, 20, 2, 1, 16, 8, 6, 9, 11]);
p13:= PermList([6, 11, 2, 5, 1, 14, 10, 3, 4, 7, 16, 9, 15, 12, 8, 13, 18, 17, 19, 20]);
p14:= PermList([4, 20, 17, 2, 5, 7, 11, 10, 1, 9, 15, 19, 13, 18, 16, 12, 3, 14, 6, 8]);
p15:= PermList([1, 17, 9, 7, 2, 8, 3, 6, 19, 14, 20, 18, 12, 11, 15, 10, 16, 4, 5, 13]);
p16:= PermList([20, 7, 8, 5, 2, 1, 3, 15, 4, 14, 16, 10, 12, 6, 19, 13, 9, 11, 17, 18]);
p17:= PermList([15, 14, 6, 19, 18, 13, 2, 5, 4, 12, 16, 3, 17, 8, 1, 20, 11, 9, 10, 7]);
p18:= PermList([2, 16, 20, 9, 18, 3, 6, 14, 7, 8, 10, 4, 17, 19, 12, 11, 5, 13, 15, 1]);
```

```
G:=Group(p0, p1, p2, p3, p4, p5, p6, p7, p8, p9, p10, p11, p12, p13, p14, p15, p16, p17, p18);
```

We can get some information about this group in a GAP session:

```
gap> Read("5pt.g");
gap> G;
<permutation group with 19 generators>
gap> StructureDescription(G);
"(C2 x C2 x C2) : S10"
gap> Blocks(G, [1..20]);
[ [ 1, 15 ], [ 2, 12 ], [ 3, 14 ], [ 4, 16 ], [ 5, 13 ], [ 6, 8 ], [ 7, 10 ], [ 9, 11 ],
[ 17, 18 ], [ 19, 20 ] ]
```

Here is a GAP function that computes the Galois width:

```
GaloisWidth := function(G)
local X, M, C, phi;
if IsTrivial(G) then return 1;
elif IsNaturalSymmetricGroup(G) or IsNaturalAlternatingGroup(G) then
X := OrbitDomain(G)[1];
if Length(X) = 4 then return 3;
else return Length(X);
fi;
elif IsCyclic(G) then return Maximum(Factors(Order(G)));
elif not IsTransitive(G) then return Maximum(List(Orbits(G), O ->
GaloisWidth(Image(ActionHomomorphism(G,O)))));
else
X := OrbitDomain(G)[1];
if not IsPrimitive(G) then
phi := ActionHomomorphism(G, Blocks(G, X), OnSets);
return Maximum(GaloisWidth(Kernel(phi)), GaloisWidth(Image(phi)));
elif IsSimple(G) then
M := List(ConjugacyClassesMaximalSubgroups(G), H -> Representative(H));
return Minimum(List(M, H -> Order(G)/Order(H)));
else
C := CompositionSeries(G);
return Maximum(List([1..Length(C)-1], i -> GaloisWidth(C[i]/C[i+1])));
fi;
fi;
end;
```

In the REPL, we get the following output:

```
gap> GaloisWidth(G);
10
```

Let me emphasize again that this calculation is largely heuristic. At best, it tells us only that the group G constructed in this example is a subgroup of the true Galois group; moreover, the path-tracking is not certified, which might call into question the veracity of some of the permutations that are constructed. Nevertheless, experience suggests that the heuristics are pretty reliable. In the case of the five-point problem, we know that the Galois width must equal 10, since 20 solutions divide into 10 blocks with constant essential matrices. Going back to Macaulay2, let's see how this information can be used to solve the problem with a 10-path homotopy. To compute the action of G on the 10 essential matrices, one may use the decomposable monodromy technique of [2]. In `MonodromySolver`, this is implemented with the option `Equivalencer` as follows:

```
W = first monodromySolve(Gs, z0, {x0}, NumberOfNodes => 5,
Equivalencer => (x -> point((matrix x)_{0,1})))
```

Here, we treat two solutions with the same t as being equivalent: note that specifying t is equivalent to specifying the left-kernel of the essential matrix.

Finally, let us demonstrate how to solve a (randomly-generated) real problem instance with parameter homotopy, using the last monodromy computation to supply the start system:

```
z0 = matrix W.BasePoint;
x0s = points W.PartialSols;
z1 = random(RR^1, RR^(numParameters Gs));
H = parametricSegmentHomotopy Gs;
H12 = specialize(H, transpose(z0 | z1));
x1s = trackHomotopy(H12, x0s);
```

This gives us 10 solutions to the target problem z_1 : the other 10 solutions may be found by applying the *twisted-pair* symmetry, representing the deck transformation group $\text{Cent}(G, S_{20}) \cong \mathbb{Z}_2$. (Note: A formula for this symmetry can be recovered using the monodromy-plus-interpolation technique proposed in [21].

```
z0 = matrix W.BasePoint;
x0s = points W.PartialSols;
z1 = random(RR^1, RR^(numParameters Gs));
H = parametricSegmentHomotopy Gs;
H12 = specialize(H, transpose(z0 | z1));
x1s = trackHomotopy(H12, x0s);
x1s = x1s | apply(x1s, x -> (
tvals := (matrix x)_{0,1};
R := transpose reshape(CC^3, CC^3, (matrix x)_{2..10});
t := transpose(tvals | matrix{1});
R2 := ((2/(transpose t*t)_{0,0}) * t * transpose t - id_(CC^3)) * R;
point(tvals | matrix{flatten entries R2})
)
);
max apply(x1s, x -> norm evaluate(G, point z1, x))
```

The last line outputs a maximum absolute residual on the order of $\approx 10^{-12}$. Please note that this is the residual for *all 15 equations*, not merely the 11 used in homotopy continuation. Thus, tracking only 10 paths suffices to recover all 20 solutions with little extra effort. In a similar manner, being able to compute the Galois groups, Galois widths, and so on has led to the new, efficient solutions of novel minimal problems surveyed here.

In conclusion, numerical monodromy computation and Galois groups offer a powerful toolkit for solving parametric systems of algebraic equations. There is more future work that can be done, e.g. concerning tailored data structures [7, 17], parallelization [5, 9, 50], and certification [22, 34, 64, 66], to name a few directions.

Overall, I feel optimistic that these techniques will continue to be used and improved—both in the setting of minimal problems surveyed here, and more broadly wherever parametric algebraic systems of equations need to be solved.

REFERENCES

- [1] Sameer Agarwal, Timothy Duff, Max Lieblich, and Rekha R Thomas. 2023. An Atlas for the Pinhole Camera. *Foundations of Computational Mathematics* (2023), 1–51.
- [2] Carlos Améndola, Julia Lindberg, and Jose Israel Rodriguez. 2016. Solving parameterized polynomial systems with decomposable projections. *arXiv preprint arXiv:1612.08807* (2016).
- [3] Federica Arrigoni, Tomás Pajdla, and Andrea Fusiello. 2023. Viewing Graph Solvability in Practice. In *IEEE/CVF International Conference on Computer Vision, ICCV 2023, Paris, France, October 1–6, 2023*. IEEE, 8113–8121. <https://doi.org/10.1109/ICCV51070.2023.00748>

[4] Daniel J Bates, Paul Breiding, Tianran Chen, Jonathan D Hauenstein, Anton Leykin, and Frank Sottile. 2023. Numerical nonlinear algebra. *arXiv preprint arXiv:2302.08585* (2023).

[5] Nathan Bliss, Timothy Duff, Anton Leykin, and Jeff Sommars. 2018. Monodromy Solver: Sequential and Parallel. In *Proceedings of the 2018 ACM on International Symposium on Symbolic and Algebraic Computation, ISSAC 2018, New York, NY, USA, July 16–19, 2018*, Manuel Kauers, Alexey Ovchinnikov, and Éric Schost (Eds.). ACM, 87–94. <https://doi.org/10.1145/3208976.3209007>

[6] Paul Breiding and Sascha Timme. 2018. HomotopyContinuation.jl: A package for homotopy continuation in Julia. In *Mathematical Software—ICMS 2018: 6th International Conference, South Bend, IN, USA, July 24–27, 2018, Proceedings*. Springer, 458–465.

[7] Taylor Brysiewicz. 2024. Monodromy Coordinates. In *International Congress on Mathematical Software*. Springer, 265–274.

[8] Taylor Brysiewicz, Jose Israel Rodriguez, Frank Sottile, and Thomas Yahl. 2021. Solving decomposable sparse systems. *Numerical Algorithms* 88, 1 (2021), 453–474. <https://doi.org/10.1007/s11075-020-01045-x>

[9] Chiang-Heng Chien, Hongyi Fan, Ahmad Abdelfattah, Elias P. Tsigaridas, Stanimire Tomov, and Benjamin B. Kimia. 2022. GPU-Based Homotopy Continuation for Minimal Problems in Computer Vision. In *IEEE/CVF Conference on Computer Vision and Pattern Recognition, CVPR 2022, New Orleans, LA, USA, June 18–24, 2022*. IEEE, 15744–15755. <https://doi.org/10.1109/CVPR52688.2022.01531>

[10] Ondřej Chum, Jiri Matas, and Josef Kittler. 2003. Locally Optimized RANSAC. In *Pattern Recognition, 25th DAGM Symposium, Magdeburg, Germany, September 10–12, 2003, Proceedings (Lecture Notes in Computer Science, Vol. 2781)*, Bernd Michaelis and Gerald Krell (Eds.). Springer, 236–243. https://doi.org/10.1007/978-3-540-45243-0_31

[11] Andrea Porfiri Dal Cin, Timothy Duff, Luca Magri, and Tomás Pajdla. 2024. Minimal Perspective Autocalibration. In *IEEE/CVF Conference on Computer Vision and Pattern Recognition, CVPR 2024, Seattle, WA, USA, June 16–22, 2024*. IEEE, 5064–5073. <https://doi.org/10.1109/CVPR52733.2024.00484>

[12] Erin Connelly, Timothy Duff, and Jessie Loucks-Tavitas. 2024. Algebra and geometry of camera resectioning. *Math. Comp.* (2024).

[13] Bernard Deconinck and Mark van Hoeij. 2001. Computing Riemann matrices of algebraic curves. Vol. 152/153. 28–46. Advances in nonlinear mathematics and science.

[14] Michel Dhome, Marc Richetin, Jean-Thierry Laprésté, and Gérard Rives. 1989. Determination of the Attitude of 3D Objects from a Single Perspective View. *IEEE Trans. Pattern Anal. Mach. Intell.* 11, 12 (1989), 1265–1278. <https://doi.org/10.1109/34.41365>

[15] Yaqing Ding, Jian Yang, Viktor Larsson, Carl Olsson, and Kalle Åström. 2023. Revisiting the P3P Problem. In *IEEE/CVF Conference on Computer Vision and Pattern Recognition, CVPR 2023, Vancouver, BC, Canada, June 17–24, 2023*. IEEE, 4872–4880. <https://doi.org/10.1109/CVPR52729.2023.00472>

[16] Timothy Duff. 2025. A Galois-Theoretic Complexity Measure for Solving Systems of Algebraic Equations. *arXiv preprint arXiv:2503.17884* (2025).

[17] Timothy Duff, Cvetelina Hill, Anders Jensen, Kisun Lee, Anton Leykin, and Jeff Sommars. 2019. Solving polynomial systems via homotopy continuation and monodromy. *IMA J. Numer. Anal.* 39, 3 (2019), 1421–1446. <https://doi.org/10.1093/imanum/dry017>

[18] Timothy Duff, Kathlén Kohn, Anton Leykin, and Tomas Pajdla. 2023. PLMP—[oint-Line Minimal Problems in Complete Multi-view Visibility. *IEEE Transactions on Pattern Analysis and Machine Intelligence* 46, 1 (2023), 421–435.

[19] Timothy Duff, Kathlén Kohn, Anton Leykin, and Tomás Pajdla. 2024. PL₁P: Point-Line Minimal Problems under Partial Visibility in Three Views. *Int. J. Comput. Vis.* 132, 8 (2024), 3302–3323. <https://doi.org/10.1007/S11263-024-01992-1>

[20] Timothy Duff, Viktor Korotynskiy, Tomas Pajdla, and Margaret H. Regan. 2022. Galois/monodromy groups for decomposing minimal problems in 3D reconstruction. *SIAM J. Appl. Algebra Geom.* 6, 4 (2022), 740–772. <https://doi.org/10.1137/21M1422872>

[21] Timothy Duff, Viktor Korotynskiy, Tomás Pajdla, and Margaret H. Regan. 2023. Using monodromy to recover symmetries of polynomial systems. In *Proceedings of the 2023 International Symposium on Symbolic and Algebraic Computation, ISSAC 2023, Tromsø, Norway, July 24–27, 2023*, Alicia Dickenstein, Elias P. Tsigaridas, and Gabriela Jeronimo (Eds.). ACM, 251–259. <https://doi.org/10.1145/3597066.3597106>

[22] Timothy Duff and Kisun Lee. [2024] ©2024. Certified homotopy tracking using the Krawczyk method. In *ISSAC'24—Proceedings of the 2024 International Symposium on Symbolic and Algebraic Computation*. ACM, New York, 274–282. <https://doi.org/10.1145/3666000.3669699>

[23] Timothy Duff and Michael Ruddy. 2023. Signatures of algebraic curves via numerical algebraic geometry. *J. Symb. Comput.* 115 (2023), 452–477. <https://doi.org/10.1016/J.JSC.2022.08.003>

[24] Timothy Duff and Felix Rydell. 2025. Metric Multiview Geometry—a Catalogue in Low Dimensions. (to appear) *Acta Universitatis Sapientiae, Mathematica* (2025).

[25] Ricardo Fabbri, Timothy Duff, Hongyi Fan, Margaret H. Regan, David da Costa de Pinho, Elias P. Tsigaridas, Charles W. Wampler, Jonathan D. Hauenstein, Peter J. Giblin, Benjamin B. Kimia, Anton Leykin, and Tomás Pajdla. 2023. Trifocal Relative Pose From Lines at Points. *IEEE Trans. Pattern Anal. Mach. Intell.* 45, 6 (2023), 7870–7884. <https://doi.org/10.1109/TPAMI.2022.3226165>

[26] Hongyi Fan, Joe Kileel, and Benjamin B. Kimia. 2023. Condition numbers in multiview geometry, instability in relative pose estimation, and RANSAC. *CoRR* abs/2310.02719 (2023). <https://doi.org/10.48550/ARXIV.2310.02719> arXiv:2310.02719

[27] Jean-Charles Faugère, Guillaume Moroz, Fabrice Rouillier, and Mohab Safey El Din. 2008. Classification of the perspective-three-point problem, discriminant variety and real solving polynomial systems of inequalities. In *Symbolic and Algebraic Computation, International Symposium, ISSAC 2008, Linz/Hagenberg, Austria, July 20–23, 2008, Proceedings*, J. Rafael Sendra and Lauroen González-Vega (Eds.). ACM, 79–86. <https://doi.org/10.1145/1390768.1390782>

[28] Martin A Fischer and Robert C Bolles. 1981. Random sample consensus: a paradigm for model fitting with applications to image analysis and automated cartography. *Commun. ACM* 24, 6 (1981), 381–395.

[29] Andrew W. Fitzgibbon. 2001. Simultaneous linear estimation of multiple view geometry and lens distortion. In *2001 IEEE Computer Society Conference on Computer Vision and Pattern Recognition (CVPR 2001), with CD-ROM, 8–14 December 2001, Kauai, HI, USA*. IEEE Computer Society, 1:125–132. <https://doi.org/10.1109/CVPR.2001.990465>

[30] Louis Gaillard and Mohab Safey El Din. 2024. Solving parameter-dependent semi-algebraic systems. In *Proceedings of the 2024 International Symposium on Symbolic and Algebraic Computation, ISSAC 2024, Raleigh, NC, USA, July 16–19, 2024*, Jonathan D. Hauenstein, Wen-shin Lee, and Shaoshi Chen (Eds.). ACM, 447–456. <https://doi.org/10.1145/3666000.3669718>

[31] André Galligo and Adrien Poteaux. 2009. Continuations and Monodromy on Random Riemann Surfaces. In *Proceedings of the 2009 Conference on Symbolic Numeric Computation (Kyoto, Japan) (SNC '09)*. Association for Computing Machinery, New York, NY, USA, 115–124. <https://doi.org/10.1145/1577190.1577210>

[32] Daniel R. Grayson and Michael E. Stillman. [n. d.]. Macaulay2, a software system for research in algebraic geometry. Available at <http://www.math.uiuc.edu/Macaulay2/>.

[33] The GAP Group. [n. d.]. GAP – Groups, Algorithms, and Programming. Available at <https://www.gap-system.org/>.

[34] Alexandre Guillemet and Pierre Lairez. [2024] ©2024. Validated numerics for algebraic path tracking. In *ISSAC'24—Proceedings of the 2024 International Symposium on Symbolic and Algebraic Computation*. ACM, New York, 36–45. <https://doi.org/10.1145/3666000.3669673>

[35] Robert M. Haralick, Chung-Nan Lee, Karsten Ottenberg, and Michael Nölle. 1994. Review and analysis of solutions of the three point perspective pose estimation problem. *Int. J. Comput. Vis.* 13, 3 (1994), 331–356. <https://doi.org/10.1007/BF02028352>

[36] Petr Hrubař, Timothy Duff, Anton Leykin, and Tomas Pajdla. 2023. Learning to Solve Hard Minimal Problems. *IEEE Transactions on Pattern Analysis and Machine Intelligence* (2023).

[37] Petr Hrubař, Timothy Duff, and Marc Pollefeys. 2024. Efficient Solution of Point-Line Absolute Pose. In *Proceedings of the IEEE/CVF Conference on Computer Vision and Pattern Recognition*. 21316–21325.

[38] Petr Hrubař, Viktor Korotynskiy, Timothy Duff, Luke Oeding, Marc Pollefeys, Tomás Pajdla, and Viktor Larsson. 2023. Four-view Geometry with Unknown Radial Distortion. In *IEEE/CVF Conference on Computer Vision and Pattern Recognition, CVPR 2023, Vancouver, BC, Canada, June 17–24, 2023*. IEEE, 8990–9000. <https://doi.org/10.1109/CVPR52729.2023.00868>

[39] Kim Kiehn, Albin Ahlbäck, and Kathlén Kohn. 2025. PLMP—Point-Line Minimal Problems for Projective SFM. (to appear) *Proceedings of ICCV 2025* (2025).

[40] Joe Kileel. 2017. Minimal Problems for the Calibrated Trifocal Variety. *SIAM J. Appl. Algebra Geom.* 1, 1 (2017), 575–598. <https://doi.org/10.1137/16M1104482>

[41] Joe Kileel and Kathlén Kohn. 2022. Snapshot of algebraic vision. *arXiv preprint arXiv:2210.11443* (2022).

[42] Viktor Kocur, Daniel Kyselica, and Zuzana Kukelova. 2024. Robust Self-Calibration of Focal Lengths from the Fundamental Matrix. In *IEEE/CVF Conference on Computer Vision and Pattern Recognition, CVPR 2024, Seattle, WA, USA, June 16–22, 2024*. IEEE, 5220–5229. <https://doi.org/10.1109/CVPR52733.2024.00499>

[43] Zuzana Kukelova, Cemal Albl, Akihiro Sugimoto, Konrad Schindler, and Tomás Pajdla. 2020. Minimal Rolling Shutter Absolute Pose with Unknown Focal Length and Radial Distortion. In *Computer Vision – ECCV 2020 – 16th European Conference, Glasgow, UK, August 23–28, 2020, Proceedings, Part V (Lecture Notes in Computer Science, Vol. 12350)*, Andrea Vedaldi, Horst Bischof, Thomas Brox, and Jan-Michael Frahm (Eds.). Springer, 698–714. https://doi.org/10.1007/978-3-030-58558-7_41

[44] Zuzana Kukelova, Jan Heller, and Andrew W. Fitzgibbon. 2016. Efficient Intersection of Three Quadrics and Applications in Computer Vision. In *2016 IEEE Conference on Computer Vision and Pattern Recognition, CVPR 2016, Las Vegas, NV, USA, June 27–30, 2016*. IEEE Computer Society, 1799–1808. <https://doi.org/10.1109/CVPR.2016.199>

[45] Zuzana Kukelova and Viktor Larsson. 2019. Radial Distortion Triangulation. In *IEEE Conference on Computer Vision and Pattern Recognition, CVPR 2019, Long Beach, CA, USA, June 16–20, 2019*. Computer Vision Foundation / IEEE, 9681–9689. <https://doi.org/10.1109/CVPR.2019.00991>

[46] Zuzana Kukelova and Tomás Pajdla. 2007. A minimal solution to the autocalibration of radial distortion. In *2007 IEEE Computer Society Conference on Computer Vision and Pattern Recognition (CVPR 2007), 18-23 June 2007, Minneapolis, Minnesota, USA*. IEEE Computer Society. <https://doi.org/10.1109/CVPR.2007.383063>

[47] Anton Leykin. 2011. Numerical algebraic geometry. *The Journal of Software for Algebra and Geometry* 3 (2011), 5–10.

[48] Anton Leykin, Jose Israel Rodriguez, and Frank Sottile. 2018. Trace test. *Arnold Math. J.* 4, 1 (2018), 113–125. <https://doi.org/10.1007/s40598-018-0084-3>

[49] Anton Leykin and Frank Sottile. 2009. Galois groups of Schubert problems via homotopy computation. *Math. Comp.* 78, 267 (2009), 1749–1765.

[50] Anton Leykin and Jan Verschelde. 2009. Decomposing solution sets of polynomial systems: a new parallel monodromy breakup algorithm. *Int. J. Comput. Sci. Eng.* 4, 2 (2009), 94–101. <https://doi.org/10.1504/IJCSCE.2009.027001>

[51] Laurentiu G. Maxim, Jose I. Rodriguez, and Botong Wang. 2020. Euclidean distance degree of the multiview variety. *SIAM Journal on Applied Algebra and Geometry* 4, 1 (2020), 28–48. <https://doi.org/10.1137/18M1233406>

[52] David Nistér, Richard I. Hartley, and Henrik Stewénius. 2007. Using Galois Theory to Prove Structure from Motion Algorithms are Optimal. In *2007 IEEE Computer Society Conference on Computer Vision and Pattern Recognition (CVPR 2007), 18-23 June 2007, Minneapolis, Minnesota, USA*. IEEE Computer Society. <https://doi.org/10.1109/CVPR.2007.383089>

[53] Mikael Persson and Klas Nordberg. 2018. Lambda Twist: An Accurate Fast Robust Perspective Three Point (P3P) Solver. In *Computer Vision - ECCV 2018 - 15th European Conference, Munich, Germany, September 8-14, 2018, Proceedings, Part IV (Lecture Notes in Computer Science, Vol. 11208)*, Vittorio Ferrari, Martial Hebert, Cristian Sminchisescu, and Yair Weiss (Eds.). Springer, 334–349. https://doi.org/10.1007/978-3-030-01225-0_20

[54] Srikumar Ramalingam, Sofien Bouaziz, and Peter F. Sturm. 2011. Pose estimation using both points and lines for geo-localization. In *IEEE International Conference on Robotics and Automation, ICRA 2011, Shanghai, China, 9-13 May 2011*. IEEE, 4716–4723. <https://doi.org/10.1109/ICRA.2011.5979781>

[55] Jürgen Richter-Gebert. 2011. *Perspectives on projective geometry*. Springer, Heidelberg. xxii+571 pages. <https://doi.org/10.1007/978-3-642-17286-1> A guided tour through real and complex geometry.

[56] Maxwell Rosenlicht. 1956. Some basic theorems on algebraic groups. *Amer. J. Math.* 78 (1956), 401–443. <https://doi.org/10.2307/2372523>

[57] Johannes L. Schönberger, Viktor Larsson, and Marc Pollefeys. 2025. Fixing the RANSAC Stopping Criterion. *CoRR* abs/2503.07829 (2025). [https://doi.org/10.48550/ARXIV.2503.07829 arXiv:2503.07829](https://doi.org/10.48550/ARXIV.2503.07829)

[58] Andrew J. Sommese, Jan Verschelde, and Charles W. Wampler. 2001. Numerical decomposition of the solution sets of polynomial systems into irreducible components. *SIAM J. Numer. Anal.* 38, 6 (2001), 2022–2046.

[59] Andrew J. Sommese and Charles W. Wampler, II. 2005. *The numerical solution of systems of polynomials*. World Scientific Publishing Co. Pte. Ltd., Hackensack, NJ. xxii+401 pages. <https://doi.org/10.1142/9789812567727> Arising in engineering and science.

[60] Frank Sottile and Thomas Yahl. 2021. Galois groups in enumerative geometry and applications. *arXiv preprint arXiv:2108.07905* (2021).

[61] Henrik Stewénius, Christopher Engels, and David Nistér. 2006. Recent developments on direct relative orientation. *ISPRS Journal of Photogrammetry and Remote Sensing* 60, 4 (2006), 284–294.

[62] Peter Sturm. 2011. A historical survey of geometric computer vision. In *International Conference on Computer Analysis of Images and Patterns*. Springer, 1–8.

[63] Bernd Sturmfels and Simon Telen. 2021. Likelihood equations and scattering amplitudes. *Algebraic Statistics* 12, 2 (2021), 167–186. <https://doi.org/10.2140/astat.2021.12.167>

[64] Joris van Der Hoeven. 2011. Reliable homotopy continuation. *Technical Report* (2011).

[65] Chi Xu, Lilian Zhang, Li Cheng, and Reinhard Koch. 2017. Pose Estimation from Line Correspondences: A Complete Analysis and a Series of Solutions. *IEEE Trans. Pattern Anal. Mach. Intell.* 39, 6 (2017), 1209–1222. <https://doi.org/10.1109/TPAMI.2016.2582162>

[66] Juan Xu, Michael Burr, and Chee Yap. 2018. An approach for certifying homotopy continuation paths: Univariate case. In *Proceedings of the 2018 ACM International Symposium on Symbolic and Algebraic Computation*. 399–406.